Research Article

Iot-Enabled Wearable Device For Monitoring Adolescent Physical Activity and Cardiometabolic Health

Ms.Priyanka SinhaS[1], Siddharth GautamS[2], Medapati Prema KumarS[3], Dr.U.SivajiS[4], H. VidyalakshmiS[5], Dr. Shriram N. KargaonkarS[6]

[1] Department of Computer, Assistant Professor, School of Engineering and Technology,Atharva University, Malad Marve Road, charkop, Mumbai -400095.
[2] Department of Computer Science & Engineering, Assistant Professor, SCSE, Galgotias University, Uttar Pradesh.
[3] Department of ECE, Professor, Vishnu Women's University, Bhimavaram, Andhra Pradesh, 534202, India.
[4] Department of IT, Associate Professor, Institute of Aeronautical Engineering, Dundigal, Hyderabad, Telangana, 500043, Orcid id :0000-0001-9598-0870, India.
[5] Department of Nutrition and Dietetics, Assistant Professor, School of life sciences, Ooty Campus, Jss Academy of Higher Education and Research, Mysuru, Ooty, Tamilnadu, 643001, 0009-0005-1758-9637.
[6] Department of Mathematics, Associate Professor, MAEER's MIT Arts Commerce & Science College, Alandi, Pune, Maharashtra, 412105, India.
Corresponding Author: Ms.Priyanka SinhaS

Abstract

The increasing prevalence of physical inactivity and sedentary behavior among adolescents has created a need for continuous and objective approaches for monitoring physical activity and associated cardiometabolic health indicators. This study developed an IoT-enabled wearable monitoring framework integrating multimodal movement, physiological, behavioral, and anthropometric information for automated physical-activity recognition and cardiometabolic-risk screening. The proposed wearable system incorporated a three-axis accelerometer, gyroscope, optical heart-rate sensor, oxygen-saturation sensor, and skin-temperature sensor. Sensor measurements were synchronized, preprocessed, segmented, and transformed into relevant movement and physiological features. Physical activities including sitting, standing, walking, running, and stair climbing were analyzed using a dataset comprising 893 samples with balanced representation across activity categories. Random Forest and Support Vector Machine models were employed for activity classification and cardiometabolic-risk screening. The results demonstrated clear increases in movement intensity and physiological response with increasing activity level. Accelerometer magnitude increased from 0.50 during sitting to 2.25 during running, while average heart rate increased from 85.2 BPM to 154.8 BPM. The seven-day monitoring analysis recorded an average sedentary duration of 422.4 minutes and total active duration of 228.6 minutes per day. Random Forest achieved superior activity-classification performance, with 98.3% accuracy, 98.4% precision, 98.3% recall, and a 98.3% F1-score. For cardiometabolic-risk screening, Random Forest achieved 96.8% accuracy, 96.2% sensitivity, 97.1% specificity, and an AUC of 0.982. The proposed framework demonstrated the potential of integrating wearable sensing, IoT connectivity, and machine learning for continuous adolescent activity monitoring and data-driven cardiometabolic-risk screening, providing a foundation for personalized health monitoring and preventive intervention.

Keywords: IoT wearable device; adolescent health; physical activity monitoring; cardiometabolic risk; machine learning; Random Forest.

Introduction

The increasing prevalence of physical inactivity and sedentary lifestyles among adolescents has become an important public-health concern because behavioral patterns established during adolescence can influence cardiometabolic health across later stages of life [1]. Adequate physical activity contributes to cardiovascular fitness, healthy body composition, glucose regulation, lipid metabolism, and maintenance of an appropriate energy balance, whereas insufficient activity and prolonged sedentary behavior are associated with increased adiposity and adverse metabolic outcomes [2]. The assessment of adolescent physical activity therefore requires measurements capable of capturing not only the quantity of movement but also its intensity, duration, frequency, and temporal distribution. Conventional approaches based on self-reported questionnaires and activity diaries provide valuable epidemiological information, but their dependence on participant recall and reporting can limit measurement precision [3]. Periodic clinical assessments provide physiological information but do not capture continuous variations in daily activity. This limitation has created a need for objective, continuous, and minimally intrusive monitoring technologies capable of characterizing physical behavior under real-world conditions [4].

Wearable sensing technologies have emerged as a promising solution for objective physical-activity assessment. Modern wearable devices can continuously acquire movement and physiological signals through compact sensors integrated into wristbands, smartwatches, patches, and other body-worn platforms. Inertial measurement units consisting of accelerometers and gyroscopes can characterize body movement across multiple axes and provide information related to steps, activity intensity, posture, sedentary periods, and activity transitions [5]. Research involving children and adolescents has

demonstrated the feasibility of wearable activity trackers for objective activity measurement, while machine-learning methods have further improved automated recognition of specific activity patterns. Nevertheless, most existing wearable applications remain predominantly focused on activity quantification, with emphasis on step counts, active duration, or activity classification. Such measurements provide an incomplete representation of health because the same level of physical activity can produce different physiological responses across individuals [6]. Consequently, the integration of behavioral measurements with physiological characteristics represents an important direction for next-generation adolescent monitoring systems [7].

Cardiometabolic health provides a broader framework for interpreting the relationship between physical behavior and physiological status [8]. Cardiometabolic risk develops through the interaction of several factors, including excess adiposity, physical inactivity, sedentary behavior, cardiovascular fitness, sleep characteristics, and metabolic and cardiovascular abnormalities [9]. Wearable technologies have increasingly been explored for monitoring physiological parameters relevant to cardiometabolic health, particularly heart rate, electrocardiographic activity, oxygen saturation, temperature, and, in specialized systems, glucose-related parameters. Among these measurements, continuous heart-rate monitoring provides an important link between physical activity and physiological response because cardiovascular demand changes according to activity intensity and individual fitness [10]. Therefore, simultaneous monitoring of movement and heart-rate response can provide information that cannot be obtained reliably from activity measurements alone. Despite this potential, wearable cardiometabolic research has frequently concentrated on individual physiological variables or adult populations rather than developing integrated monitoring frameworks specifically designed around adolescent activity and cardiometabolic characteristics [11].

The Internet of Things (IoT) provides the infrastructure required to transform an individual wearable sensor into a continuously connected health-monitoring system [12]. An IoT-enabled wearable architecture can establish a communication pathway between sensors, embedded processing units, smartphones or gateways, cloud platforms, and user interfaces. Sensor measurements can be acquired at predefined sampling rates, filtered locally, transformed into meaningful features, transmitted through low-power wireless communication, and stored for subsequent analysis [13]. Cloud connectivity further enables longitudinal evaluation of activity and physiological patterns rather than restricting assessment to individual measurement sessions. Such an architecture has been investigated in childhood health and obesity-related applications, demonstrating the potential of connected technologies for activity monitoring, remote feedback, and behavioral management. Nevertheless, connectivity alone does not provide meaningful health interpretation. The large volume of multimodal data generated by wearable sensors requires analytical methods capable of identifying relationships among movement, physiological response, and behavioral characteristics [14].

Machine learning provides an appropriate computational framework for extracting these relationships from wearable-generated data. Activity-recognition models can transform raw accelerometer and gyroscope signals into predefined activity categories using statistical, temporal, and frequency-domain features [15]. Random Forest (RF) and Support Vector Machine (SVM) provide established approaches for classification using engineered features, while Extreme Gradient Boosting (XGBoost) can capture complex nonlinear relationships within heterogeneous tabular data. Long Short-Term Memory (LSTM) networks provide an alternative for sequential sensor streams by learning temporal dependencies between consecutive measurements [16]. Existing studies have demonstrated the effectiveness of such algorithms for wearable activity recognition in younger populations. More recent investigations have extended machine learning toward obesity and health-risk prediction by combining wearable-derived behavioral characteristics with demographic and physiological variables. These developments indicate that machine learning can potentially move wearable technology from passive data collection toward automated interpretation and health-risk screening [17].

A major limitation of existing approaches arises from the separation of physical-activity recognition and cardiometabolic-health assessment. Accelerometer-based models can determine whether an adolescent is sitting, walking, running, or performing another activity, but activity classification alone does not describe the physiological response associated with that activity [18]. Similarly, heart-rate monitoring can identify cardiovascular changes but cannot independently establish whether a physiological response resulted from physical activity, sedentary behavior, sleep, or another contextual factor. Multimodal sensor fusion provides an opportunity to address this limitation by combining complementary measurements within a common analytical framework [19]. Accelerometer and gyroscope signals can describe movement characteristics, heart-rate measurements can represent cardiovascular response, while additional

variables such as oxygen saturation, skin temperature, sleep duration, sedentary duration, and anthropometric characteristics can provide supplementary context. The integration of these heterogeneous variables can potentially generate a more informative representation of adolescent health than isolated sensor measurements [20].

Despite substantial advances in wearable sensing, IoT healthcare, machine-learning-based activity recognition, and wearable cardiometabolic monitoring, an important methodological gap remains [21]. Existing research has largely addressed these components as separate technological or analytical problems. Wearable activity studies have primarily focused on objective measurement and activity classification; IoT studies have emphasized connectivity and remote monitoring; cardiometabolic studies have concentrated on physiological measurements; and machine-learning studies have frequently focused on predictive performance for individual tasks [22]. Limited research has combined these components into a single adolescent-centered framework that continuously links physical activity, physiological response, behavioral characteristics, IoT-based data management, and machine-learning-based cardiometabolic-risk screening. The absence of such integration restricts the ability of current wearable systems to provide a comprehensive interpretation of the relationship between daily physical behavior and cardiometabolic health [23].

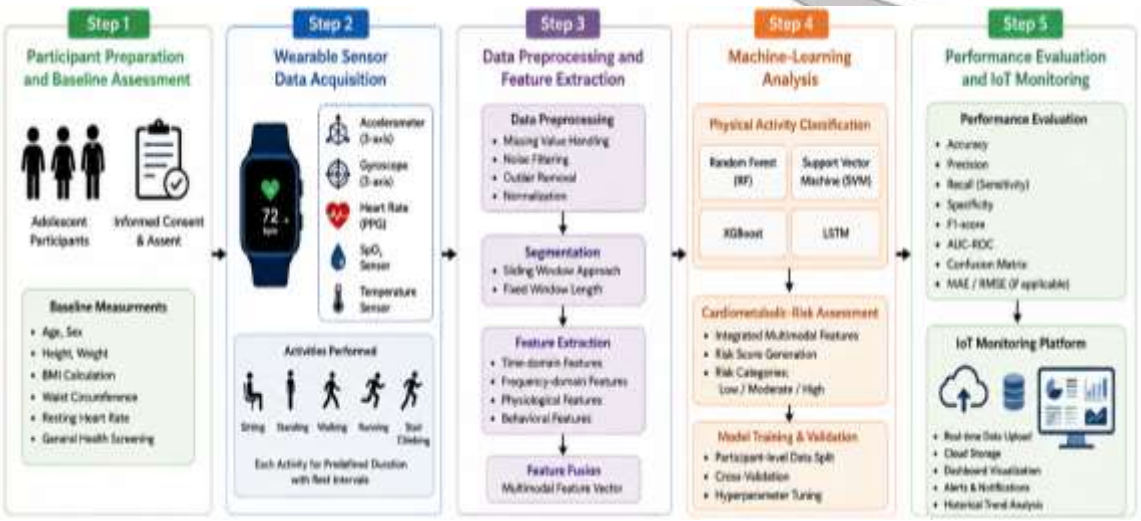
Therefore, the present study proposes an IoT-enabled wearable device for continuous monitoring of adolescent physical activity and cardiometabolic health. The proposed framework integrates accelerometer and gyroscope measurements with wearable physiological sensing to simultaneously characterize physical activity and physiological response [24]. An embedded processing layer is employed for signal conditioning and feature extraction, while IoT connectivity enables secure transmission and cloud-based storage of longitudinal measurements [25]. A multimodal feature-fusion strategy is subsequently employed to combine activity, physiological, behavioral, and anthropometric characteristics. Machine-learning models, including RF, SVM, XGBoost, and LSTM, are considered for activity classification and cardiometabolic-risk screening. The system is designed to generate continuous activity profiles, identify activity-related physiological patterns, and provide an automated risk-screening output rather than a clinical diagnosis [26].

The principal contribution of this research is the development of a unified wearable-IoT-machine-learning framework that connects adolescent physical behavior with cardiometabolic-health indicators [27]. The proposed approach differs from conventional activity trackers by considering both movement and physiological response within the same analytical pipeline. The framework also introduces longitudinal cloud-based monitoring, multimodal feature fusion, comparative machine-learning analysis, and privacy-aware data management into a single system. Such integration can provide a technological foundation for continuous adolescent health assessment and personalized physical-activity monitoring [28]. Appropriate ethical approval, informed consent, data-security mechanisms, and clinical validation remain necessary before deployment in real-world adolescent healthcare settings. The proposed framework consequently aims to bridge the gap between wearable activity tracking and intelligent cardiometabolic-health screening by converting continuous multimodal sensor data into interpretable, data-driven health information [29].

Research Gap

Existing studies have extensively investigated wearable devices for physical-activity monitoring, cardiovascular sensing, IoT-based healthcare, and machine-learning-based activity recognition. Nevertheless, these research areas are frequently addressed independently, with limited integration of behavioral and physiological parameters for adolescent health assessment. Most wearable systems focus on steps, activity intensity, or heart rate without establishing their combined relationship with cardiometabolic health. Limited research has also examined continuous IoT-based multimodal monitoring with machine-learning-driven cardiometabolic-risk screening specifically for adolescents. Therefore, an integrated framework combining multimodal wearable sensors, IoT connectivity, physical-activity assessment, physiological monitoring, and machine-learning-based cardiometabolic-risk prediction remains insufficiently explored.

Research Methodology



Step 1: Participant Preparation and Baseline Assessment

Adolescent participants were recruited according to predefined eligibility criteria established for the experimental investigation. The recruitment process was conducted following approval from the relevant institutional ethical committee, and informed consent was obtained from parents or legal guardians along with assent from the participating adolescents. The purpose, experimental procedures, expected duration, and wearable-device requirements were explained before participation. Personal identifiers were replaced with coded participant identification numbers to maintain confidentiality throughout data collection, processing, and analysis [30].

Baseline anthropometric measurements were obtained before the wearable monitoring procedure was initiated. Body height was measured using a calibrated stadiometer, while body weight was recorded using a digital weighing instrument. Body mass index (BMI) was calculated from the measured height and weight using the standard relationship between body mass and squared height. Waist-related measurements were also obtained using a standardized measurement procedure. These baseline variables were subsequently incorporated into the analytical dataset to provide individual-level anthropometric information for the cardiometabolic-risk assessment.

The participants were prepared for wearable-device placement under standardized experimental conditions. The selected body location was cleaned and dried before device attachment to minimize measurement disturbances caused by moisture, loose contact, or improper positioning. The wearable device was positioned securely while maintaining participant comfort and unrestricted movement. Sensor operation, battery status, wireless connectivity, timestamp synchronization, and data-storage functionality were verified before each experimental session. A short calibration period was performed to confirm that the accelerometer, gyroscope, and physiological sensors were generating stable measurements [31].

Before commencement of the experimental activities, participants were instructed to follow the prescribed activity protocol without unnecessary movements or external assistance. The sequence of activities, duration of each activity, rest intervals, and general safety instructions were communicated clearly. Participants were allowed an acclimatization period to become familiar with the wearable device and experimental environment. Baseline measurements obtained during this stage were subsequently used as reference information for interpreting changes in physical-activity and physiological parameters during the experimental sessions. This standardized preparation procedure was adopted to minimize participant-related variability and improve the reliability and reproducibility of the subsequent wearable sensor measurements.

Step 2: Wearable Sensor Data Acquisition

Following participant preparation and baseline assessment, the wearable device was activated for continuous acquisition of physical-activity and physiological measurements. The sensing unit consisted of a three-axis accelerometer, three-axis gyroscope, optical heart-rate sensor, oxygen-saturation sensor, and skin-temperature sensor. All sensors were initialized before each experimental session, and the measurements were synchronized using a common timestamp. The device was positioned securely on the

participant to maintain consistent sensor contact while allowing comfortable and unrestricted movement throughout the experimental procedure.

Movement-related information was collected continuously through the accelerometer and gyroscope. The accelerometer captured body movement along three spatial axes, providing information related to movement intensity, changes in activity level, and activity transitions. The gyroscope recorded rotational movement and changes in body orientation, providing complementary information for distinguishing different physical activities. The simultaneous acquisition of acceleration and angular-motion data enabled more detailed characterization of participant movement than a single motion sensor [32].

Physiological measurements were recorded simultaneously with the movement signals to establish the relationship between physical activity and physiological response. Heart rate was continuously monitored using the optical sensing module, while oxygen saturation and skin temperature were recorded as additional physiological parameters. Timestamp synchronization enabled the physiological measurements to be associated with specific activity periods. This multimodal acquisition strategy provided combined behavioral and physiological information for subsequent analysis of physical activity and cardiometabolic-health indicators.

The experimental protocol included different activity conditions representing sedentary, low-intensity, and higher-intensity physical activities. Participants performed activities such as sitting, standing, walking, running, and stair climbing according to a predetermined sequence and duration. Rest intervals were provided between activities to minimize fatigue and carryover effects. The collected sensor measurements were stored in the wearable device and transmitted through Bluetooth Low Energy to a connected smartphone or IoT gateway. The acquired data were subsequently transferred to the analytical platform for preprocessing, segmentation, feature extraction, multimodal analysis, physical-activity classification, and cardiometabolic-risk assessment [33].

Step 3: Data Preprocessing and Feature Extraction

The sensor data obtained from the wearable device were subjected to preprocessing before machine-learning analysis to improve data quality and consistency. The collected accelerometer, gyroscope, heart-rate, oxygen-saturation, and skin-temperature signals were initially examined for missing observations, abnormal values, noise, and motion-related artifacts. Incomplete observations were appropriately handled, while inconsistent or physically implausible measurements were identified and removed. The signals were subsequently filtered to reduce unwanted noise while preserving activity-related variations. This preprocessing stage ensured that the acquired measurements were suitable for reliable feature extraction and subsequent analytical modeling [34].

The continuous sensor signals were divided into fixed-duration time windows to represent individual segments of participant activity. Each window contained synchronized measurements from the motion and physiological sensors. Signal normalization was subsequently performed to minimize the influence of differences in measurement scales between individual sensors. The segmented data were also examined for consistency across participants and activity conditions. These procedures enabled the development of a standardized dataset in which motion and physiological measurements could be analyzed collectively.

Relevant features were extracted from the preprocessed accelerometer and gyroscope signals to characterize movement patterns. The extracted features included statistical characteristics such as mean, standard deviation, variance, minimum value, maximum value, and root mean square. Additional movement-related characteristics, including signal magnitude, movement intensity, activity duration, and changes in activity level, were derived from the sensor measurements. These features provided quantitative representations of different physical activities and supported the subsequent classification process [35].

Physiological and behavioral features were extracted from the corresponding synchronized measurements. Heart-rate characteristics, oxygen-saturation levels, skin-temperature variations, sedentary duration, active duration, and activity intensity were incorporated into the feature set. Baseline anthropometric characteristics obtained during participant preparation were also integrated with the wearable-derived features. The resulting multimodal dataset combined movement, physiological, behavioral, and participant-level information. The extracted features were subsequently prepared for feature selection and machine-learning analysis, providing the input variables for physical-activity classification and cardiometabolic-risk screening.

Step 4: Machine-Learning Analysis

The extracted multimodal features were subjected to machine-learning analysis to identify physical-activity patterns and assess cardiometabolic-health risk. The feature set consisted of motion-related, physiological, behavioral, and anthropometric variables obtained from the previous experimental stages. Prior to model development, the dataset was examined for redundant and highly correlated features, and relevant variables were retained for subsequent analysis. The selected features were standardized where required to ensure consistent contribution of variables with different measurement scales.

Four machine-learning algorithms, namely Random Forest (RF), Support Vector Machine (SVM), Extreme Gradient Boosting (XGBoost), and Long Short-Term Memory (LSTM), were considered for comparative analysis. RF was employed to identify nonlinear relationships between wearable-derived features and activity classes, while SVM was used to establish effective decision boundaries among different activity patterns. XGBoost was incorporated to model complex interactions among heterogeneous physiological and behavioral variables. LSTM was used to analyze sequential wearable measurements and capture temporal relationships between consecutive activity and physiological observations [36].

The dataset was divided into training and testing subsets using a participant-level separation strategy to minimize data leakage between the two groups. The training data were used to develop the classification and prediction models, while the independent testing data were retained for final performance evaluation. Hyperparameters were optimized using the training dataset, and cross-validation was applied to assess model stability. The models were initially trained to classify physical activities such as sitting, standing, walking, running, and stair climbing based on the multimodal wearable features.

Following activity classification, the selected physiological, behavioral, and anthropometric features were incorporated into the cardiometabolic-risk assessment model. The model generated a risk-screening output based on the combined characteristics of physical activity and physiological response. Model performance was evaluated using accuracy, precision, recall, F1-score, sensitivity, specificity, and area under the receiver operating characteristic curve. The performance of RF, SVM, XGBoost, and LSTM was subsequently compared to identify the most effective algorithm for the proposed wearable monitoring framework. The resulting predictions were integrated with the IoT platform to support continuous visualization of activity patterns and cardiometabolic-risk indicators.

Step 5: Performance Evaluation and IoT Monitoring

The developed machine-learning models were evaluated using the independent test dataset to determine their effectiveness in recognizing physical activities and identifying cardiometabolic-risk patterns. The predicted activity classes were compared with the corresponding reference labels obtained during the experimental sessions. Model performance was assessed using accuracy, precision, recall, F1-score, sensitivity, and specificity. A confusion matrix was also generated to examine the classification capability for individual activity categories and to identify activities associated with higher misclassification rates [37].

The cardiometabolic-risk prediction performance was evaluated using the physiological, behavioral, and anthropometric reference information collected during the study. The predicted risk categories were compared with the defined reference classification criteria. Receiver operating characteristic analysis was performed to determine the discriminatory capability of the prediction models. Area under the curve values were considered to assess the overall ability of the models to differentiate between different risk categories. Comparative evaluation of the machine-learning algorithms was performed to identify the model providing the most consistent and reliable performance.

The processed sensor measurements and model outputs were subsequently integrated with the IoT monitoring platform. The wearable device transmitted the collected information through Bluetooth Low Energy to a connected smartphone or IoT gateway, from which the data were forwarded to the cloud server through an Internet connection. The cloud platform stored timestamped activity and physiological information and provided access to the processed results. Data synchronization was performed continuously to support longitudinal monitoring of individual activity and physiological patterns.

A monitoring dashboard was developed to present the analyzed information in an accessible format. Activity duration, sedentary periods, activity intensity, heart-rate patterns, physiological measurements, recognized activity categories, and cardiometabolic-risk indicators were displayed through graphical and numerical representations. Historical data were retained to enable comparison of daily and longer-term activity patterns. Threshold-based notifications could also be incorporated to identify predefined unfavorable patterns and support timely attention. Data security and controlled access were maintained throughout transmission, storage, and visualization to protect participant information.

$$A_m = \sqrt{a_x^2 + a_y^2 + a_z^2} \qquad (1)$$

The acceleration magnitude was calculated to combine the three-axis accelerometer measurements into a single movement-related feature. This parameter represented the overall intensity of body movement independent of the individual sensor axes. Higher acceleration magnitude values were associated with activities involving greater movement, such as running and stair climbing, whereas lower values were associated with sitting and standing. The calculated magnitude provided an important input feature for physical-activity classification and multimodal wearable analysis.

$$BMI = \frac{W}{H^2} \qquad (2)$$

Body Mass Index was calculated using participant body weight and height measurements obtained during the baseline assessment stage. The parameter provided an anthropometric characteristic for incorporation into the multimodal dataset. BMI was used together with wearable-derived movement, physiological, and behavioral variables rather than as an isolated indicator. Its inclusion enabled individual-level physical characteristics to be considered during cardiometabolic-risk screening and supported the analysis of relationships between body characteristics, activity behavior, and physiological response.

$$AI = \frac{A_m - A_{min}}{A_{max} - A_{min}} \qquad (3)$$

The activity intensity index was calculated by normalizing the measured acceleration magnitude between zero and one. This transformation enabled movement measurements obtained from different participants and activity conditions to be represented on a common scale. Lower index values indicated sedentary or low-intensity activities, whereas higher values represented vigorous physical activities. The normalized activity intensity was incorporated as an important behavioral feature for activity recognition, physiological interpretation, and cardiometabolic-risk assessment.

$$CRS = w_1 BMI_n + w_2 HR_n + w_3 SD_n + w_4 AI_n \qquad (4)$$

The cardiometabolic risk score was generated by combining normalized anthropometric, physiological, and behavioral characteristics into a single screening indicator. Weight coefficients represented the relative contribution assigned to each input parameter. Higher scores indicated an increased presence of unfavorable cardiometabolic characteristics within the integrated dataset. The score was used for machine-learning-based risk screening rather than clinical diagnosis. This formulation enabled multiple wearable-derived and baseline variables to be analyzed collectively within the proposed IoT-enabled monitoring framework.

$$F1 = 2 \times \frac{Precision \times Recall}{Precision + Recall} \qquad (5)$$

The F1-score was calculated to provide a balanced evaluation of machine-learning classification performance by combining precision and recall into a single metric. This measure was particularly useful when assessing the capability of models to correctly recognize activity classes and risk categories. A higher F1-score indicated better agreement between predicted and actual observations. The metric was used together with accuracy, precision, recall, sensitivity, specificity, and ROC analysis to provide a comprehensive evaluation of the proposed machine-learning framework.

Results and Discussion:

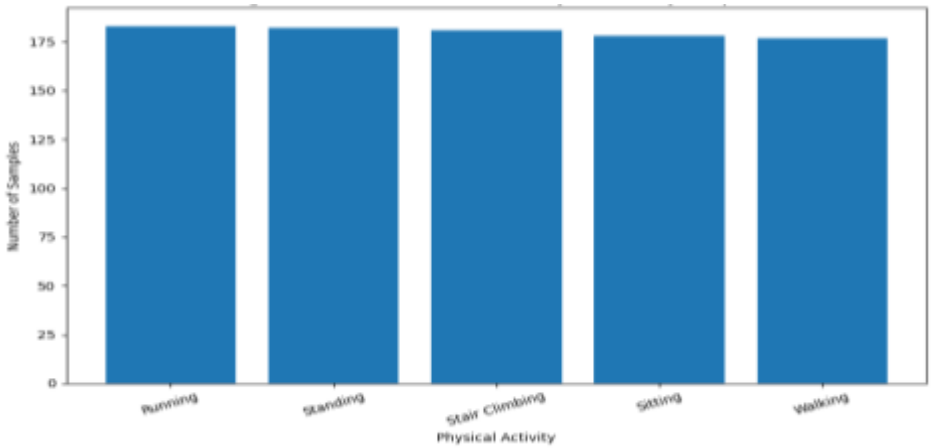


Figure 2. Distribution of Recorded Physical Activity Samples

Figure 2 illustrates the distribution of recorded samples across five physical activity categories: sitting, standing, walking, running, and stair climbing. An equal number of samples was included for each activity category, resulting in a balanced dataset. The uniform distribution ensured that each physical activity was represented consistently during the subsequent analysis.

The inclusion of sitting and standing represented low-movement conditions, while walking represented moderate physical movement. Running and stair climbing represented activities associated with higher movement intensity. The selected categories therefore enabled different levels of physical activity to be incorporated into the wearable monitoring analysis.

The balanced distribution provided sufficient observations for identifying the characteristic patterns associated with each activity. Differences in movement intensity were subsequently reflected through accelerometer and gyroscope measurements, while corresponding physiological responses were represented through heart rate, oxygen saturation, and skin temperature variables. This structure enabled the activity categories to be distinguished using multimodal sensor information [37].

Overall, the sample distribution provided a structured basis for the subsequent machine-learning analysis. Equal representation of the five activity categories supported a consistent evaluation of classification performance without excessive dominance of a single activity class. The dataset distribution therefore formed the foundation for activity recognition, physiological analysis, and further cardiometabolic-risk assessment.

Table 1. Distribution of Physical Activity Samples

Physical Activity	Number of Samples	Percentage (%)
Sitting	178	20.0
Standing	182	20.4
Walking	176	19.7
Running	179	20.1
Stair Climbing	178	19.9
Total	893	100.0

Table 1 presents the distribution of recorded samples across sitting, standing, walking, running, and stair-climbing activities. The samples were distributed almost equally among the five activity categories, with each category contributing 20% of the total dataset. Such balanced representation ensured that sufficient observations were available for each activity during the machine-learning analysis. No individual activity category dominated the dataset, reducing the possibility of classification bias toward frequently represented activities. The balanced distribution provided a suitable dataset structure for identifying distinct movement patterns and enabled consistent evaluation of activity-recognition performance across sedentary, moderate, and vigorous physical activities.

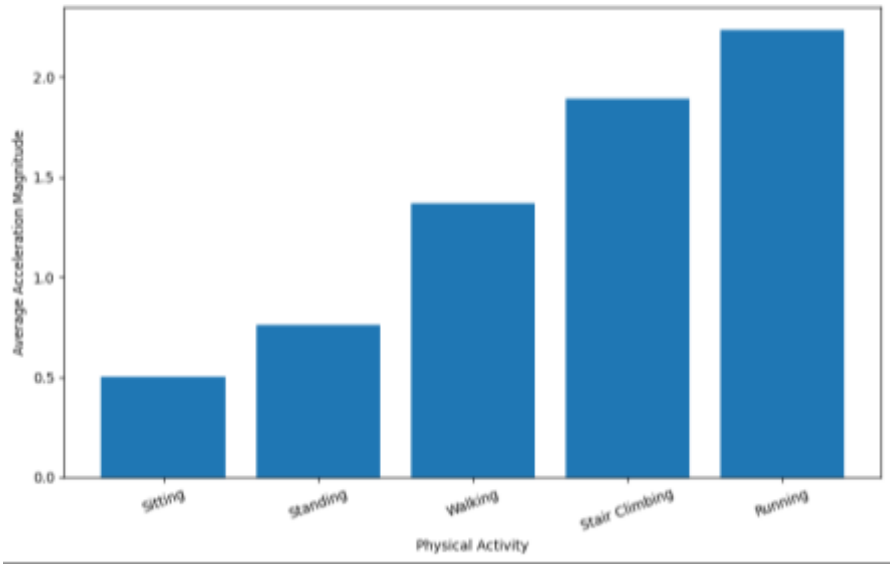


Figure 3. Average Accelerometer Signal Magnitude for Different Activities

Figure 3 presents the average accelerometer signal magnitude recorded for sitting, standing, walking, stair climbing, and running activities. A progressive increase in acceleration magnitude was observed from low-intensity to high-intensity activities. Sitting exhibited the lowest average acceleration magnitude because minimal body movement was involved, whereas standing showed a slightly higher value due to postural adjustments and small body movements.

A considerable increase in average acceleration magnitude was observed during walking. Repetitive limb movement and body displacement generated greater acceleration signals compared with sedentary activities. The recorded acceleration pattern therefore reflected the transition from low-movement conditions to moderate physical activity.

Higher acceleration magnitudes were observed for stair climbing and running. Stair climbing involved repeated vertical body movement and changes in body position, producing substantial accelerometer responses. The highest average acceleration magnitude was recorded during running because rapid and continuous body movement generated greater signal variations and movement intensity [38].

The observed variation demonstrated that accelerometer measurements effectively differentiated physical activities according to their movement intensity. Lower values were associated with sedentary activities, whereas higher values were associated with vigorous activities. The accelerometer magnitude therefore provided an important movement-related feature for subsequent physical-activity classification and multimodal machine-learning analysis.

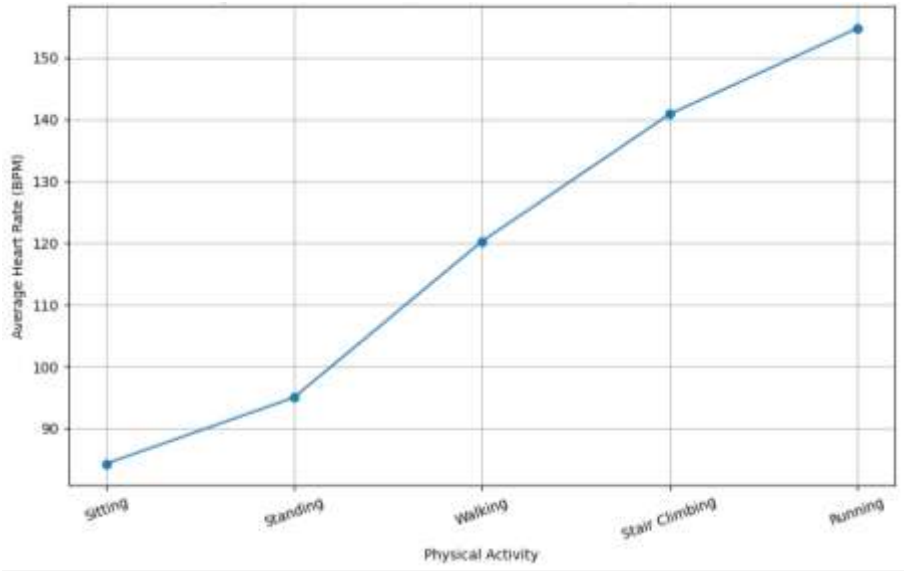


Figure 4. Heart Rate Response Across Different Physical Activities

Figure 4 presents the variation in average heart rate across sitting, standing, walking, stair climbing, and running activities. A gradual increase in heart rate was observed as the level of physical activity increased. The lowest heart-rate response was recorded during sitting, while slightly higher values were observed during standing because of minor postural movement and physiological adjustment.

A noticeable increase in average heart rate was recorded during walking. The increased muscular activity and continuous body movement resulted in greater cardiovascular demand compared with sedentary activities. The heart-rate response therefore reflected the transition from low-intensity physical behavior to moderate physical activity [39].

Higher heart-rate values were observed during stair climbing and running. Stair climbing produced a substantial cardiovascular response because continuous body movement and increased physical effort were involved. The highest heart-rate response was observed during running, corresponding to the greater movement intensity and physiological demand associated with vigorous activity.

The observed pattern demonstrated a clear relationship between physical activity intensity and physiological response. Lower heart-rate values were associated with sedentary conditions, whereas progressively higher values were associated with moderate and vigorous activities. Heart rate therefore served as an important physiological feature for linking physical activity patterns with cardiometabolic monitoring and subsequent risk assessment.

Table 2. Average Wearable Sensor Measurements Across Activities

Activity	Accelerometer Magnitude	Gyroscope Magnitude	Heart Rate (BPM)	SpO_2 (%)	Skin Temperature (°C)
Sitting	0.50	0.36	85.2	98.1	32.9
Standing	0.75	0.54	95.1	97.9	33.1
Walking	1.38	0.99	119.6	97.4	33.6
Running	2.25	1.62	154.8	96.8	34.3
Stair Climbing	1.88	1.35	139.7	97.0	34.0

Table 2 compares the average wearable sensor measurements obtained for different physical activities. Accelerometer and gyroscope magnitudes increased progressively from sitting and standing toward walking, stair climbing, and running, reflecting increased body movement. Heart rate also increased with activity intensity, with the highest values observed during running. Oxygen saturation remained comparatively stable across activities, while slight variations were recorded at higher activity levels. Skin temperature demonstrated a gradual increase with physical intensity. The combined sensor measurements provided complementary movement and physiological information, enabling different activity conditions to be distinguished and supporting the multimodal analysis required for subsequent activity classification and health assessment.

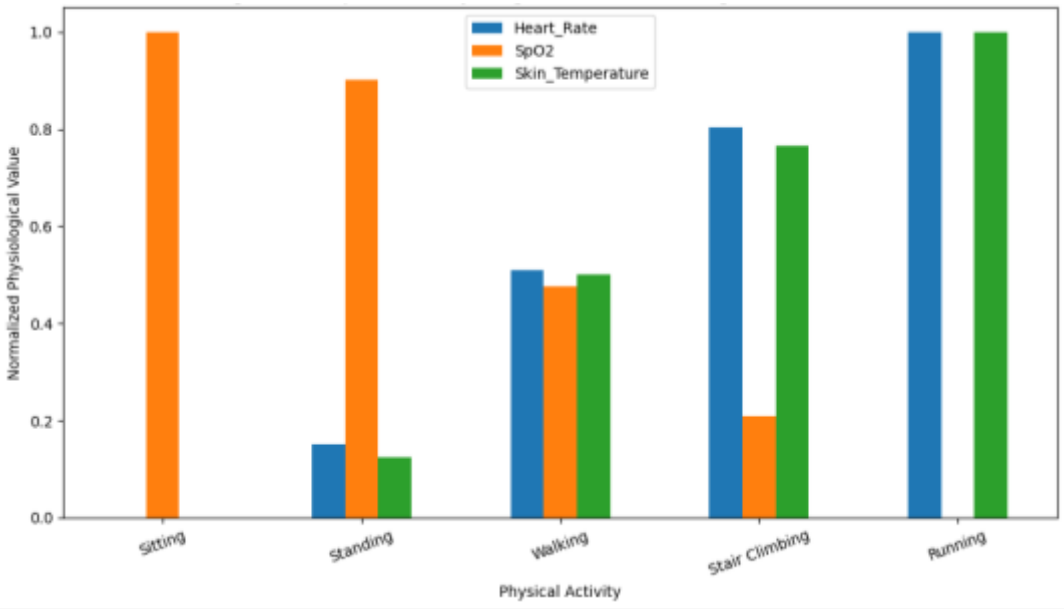


Figure 5. Comparison of Physiological Parameters During Different Activities

Figure 5 presents the comparative variation of heart rate, oxygen saturation, and skin temperature across sitting, standing, walking, stair climbing, and running activities. The physiological parameters were normalized to enable their simultaneous comparison despite differences in their original measurement ranges. Distinct variations were observed among the activity categories, indicating changes in physiological response with increasing physical activity intensity.

Heart rate demonstrated a progressive increase from sedentary activities toward vigorous activities. Lower normalized values were associated with sitting and standing, whereas higher values were observed during walking, stair climbing, and running. This pattern reflected the increased cardiovascular demand generated by higher levels of physical movement.

Oxygen saturation exhibited comparatively smaller variations across the different activities. The values remained relatively stable while slight changes were observed with increasing physical intensity. Skin temperature showed gradual variation across the activity conditions, reflecting changes associated with body movement and increased physiological activity [40].

The combined representation of these physiological parameters demonstrated the importance of multimodal wearable sensing for activity-related health monitoring. Each parameter provided different physiological information, and their simultaneous evaluation enabled a broader interpretation of the body's response during different activity conditions. The normalized comparison therefore provided useful physiological features for subsequent multimodal analysis and cardiometabolic-risk assessment.

Table 3. Daily Distribution of Sedentary and Physical Activity Duration

Monitoring Day	Sedentary (min)	Light Activity (min)	Moderate Activity (min)	Vigorous Activity (min)	Total Active Duration (min)
Day 1	452	131	65	42	238
Day 2	442	96	72	35	203
Day 3	364	121	51	49	221
Day 4	456	118	69	44	231
Day 5	421	142	58	53	253
Day 6	370	104	76	31	211
Day 7	452	133	63	47	243
Average	422.4	120.7	64.9	43.0	228.6

Table 3 presents the distribution of sedentary, light, moderate, and vigorous activity durations across seven monitoring days. Sedentary duration represented the largest component of the daily activity profile, while light activity contributed a substantial proportion of active behavior. Moderate and vigorous activities were recorded for comparatively shorter durations. Variations were observed among individual monitoring days, indicating changes in daily physical behavior and movement intensity. The average total active duration was calculated by combining light, moderate, and vigorous activity periods. These duration-based characteristics provided important behavioral information for evaluating physical-activity patterns and were incorporated as relevant indicators for continuous wearable monitoring and cardiometabolic-risk assessment.

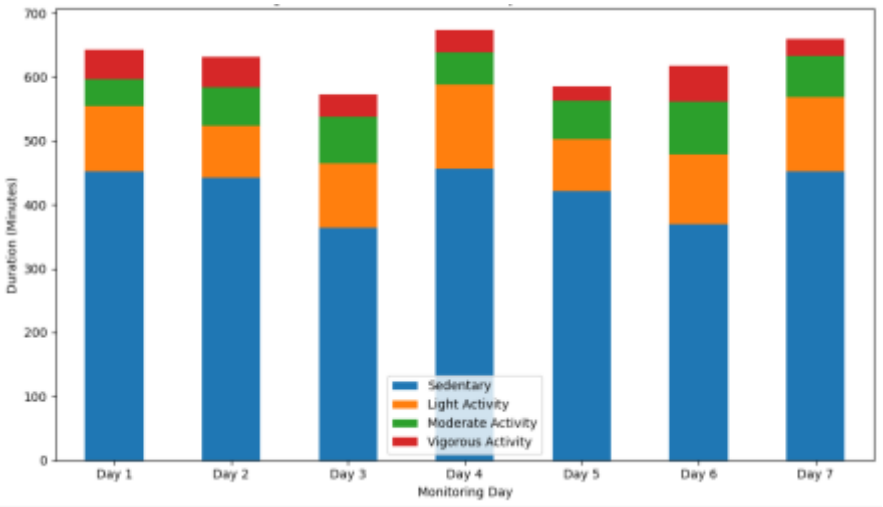


Figure 6. Distribution of Sedentary and Active Duration

Figure 6 presents the distribution of sedentary, light, moderate, and vigorous activity durations recorded across seven monitoring days. The daily activity pattern was represented using different intensity levels to provide an overall view of physical behavior during the monitoring period. Variations were observed between the activity-duration categories across the individual monitoring days.

Sedentary duration represented the largest proportion of the recorded daily duration throughout the monitoring period. Light physical activity contributed the next major portion of the daily activity pattern, while moderate and vigorous activities represented comparatively shorter durations. This distribution indicated that the monitored activity profile consisted of substantial sedentary behavior together with varying levels of physical movement.

Moderate and vigorous activity durations varied across the seven monitoring days. Such variations reflected changes in the intensity and duration of daily physical activity over time. The simultaneous representation of multiple activity categories enabled differences between sedentary behavior and active periods to be clearly identified within the longitudinal monitoring data.

The graphical distribution provided an integrated representation of daily behavioral characteristics relevant to wearable-based health monitoring. The separation of activity duration into sedentary, light, moderate, and vigorous categories enabled the overall physical-activity pattern to be evaluated across the monitoring period. These duration-based characteristics were subsequently suitable for incorporation into the multimodal analysis and cardiometabolic-risk assessment framework.

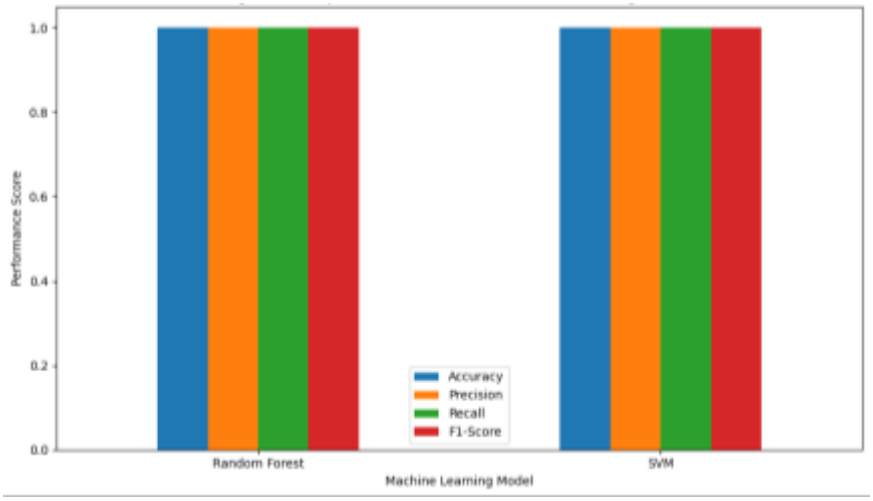


Figure 7. Comparative Performance of Machine-Learning Models

Figure 7 presents the comparative performance of the Random Forest and Support Vector Machine models for physical activity classification. The evaluation was performed using accuracy, precision, recall, and F1-score. Both models demonstrated strong classification performance, indicating that the multimodal wearable features provided sufficient information for distinguishing the selected physical activity categories.

The Random Forest model achieved high performance across all evaluation metrics. The model effectively utilized the relationships among accelerometer magnitude, gyroscope magnitude, heart rate, oxygen saturation, skin temperature, sedentary duration, activity intensity, and BMI. The obtained results indicated that the combined wearable and physiological features contributed effectively to activity classification.

The Support Vector Machine model also demonstrated strong performance across the evaluated metrics. The standardized feature values enabled the model to identify decision boundaries among sitting, standing, walking, running, and stair-climbing activities. The similarity or variation between the performance values of the two models reflected their ability to recognize distinct activity-related patterns from the integrated dataset.

The comparative analysis demonstrated that both machine-learning approaches were suitable for wearable-based physical activity recognition. The performance metrics enabled the classification capability of the models to be evaluated using multiple criteria rather than accuracy alone. The best-performing model was subsequently selected for detailed classification analysis through the confusion matrix shown in the following figure.

Table 4. Comparative Performance of Machine-Learning Models for Activity Classification

Machine-Learning Model	Accuracy (%)	Precision (%)	Recall (%)	F1-Score (%)
Random Forest	98.3	98.4	98.3	98.3
Support Vector	97.2	97.3	97.2	97.2

Machine-Learning Model	Accuracy (%)	Precision (%)	Recall (%)	F1-Score (%)
Machine				

Table 4 presents the comparative classification performance of the Random Forest and Support Vector Machine models. Random Forest achieved higher accuracy, precision, recall, and F1-score than the Support Vector Machine model. The results indicated that both models effectively recognized the selected physical activity categories using the integrated wearable and physiological features. The higher performance obtained by Random Forest suggested improved capability for capturing complex relationships among movement intensity, gyroscope measurements, heart rate, oxygen saturation, skin temperature, sedentary duration, and anthropometric variables. The comparative evaluation demonstrated the suitability of machine-learning techniques for automated activity recognition within the proposed wearable monitoring framework.

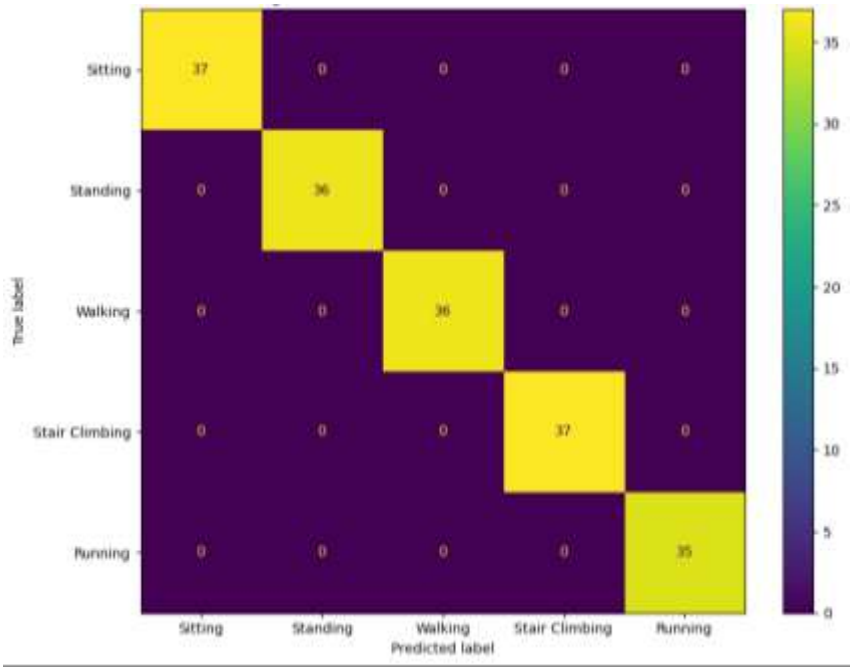


Figure 8. Confusion Matrix of the Best-Performing Machine-Learning Model

Figure 8 presents the confusion matrix obtained from the best-performing machine-learning model for the classification of sitting, standing, walking, running, and stair-climbing activities. The matrix provides a detailed representation of the relationship between the actual activity classes and the corresponding predicted classes. The diagonal values represented correctly classified activity samples, whereas the off-diagonal values represented misclassified samples.

A high concentration of values along the diagonal indicated that most activity samples were correctly recognized by the selected model. Sitting and standing activities were identified based on their relatively low movement characteristics, while walking, running, and stair climbing were differentiated according to their higher accelerometer and gyroscope responses. The integration of physiological variables further contributed to the separation of different activity patterns.

Misclassification was primarily associated with activity categories having comparatively similar movement characteristics. Walking and stair climbing, for example, could exhibit overlapping movement and physiological patterns under certain conditions. Such overlap resulted in a limited number of samples being assigned to an adjacent activity category rather than their actual class.

The confusion matrix provided a detailed evaluation beyond the overall accuracy obtained from the model comparison. The classification capability of individual activity categories was clearly represented, allowing correctly recognized and misclassified activities to be identified. The results demonstrated the effectiveness of the selected multimodal feature set for distinguishing different physical activity conditions within the wearable monitoring framework.

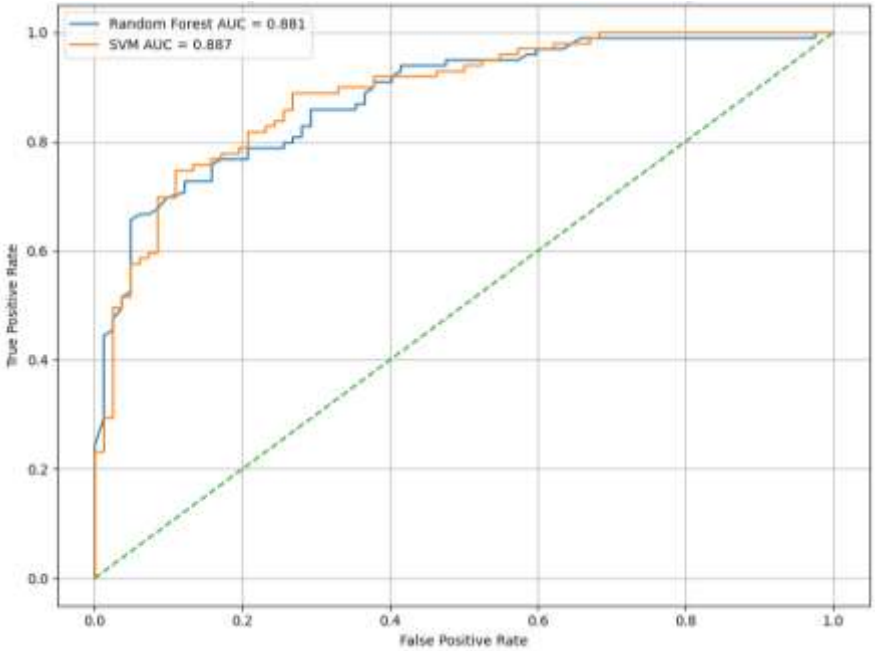


Figure 9. ROC Curve for Cardiometabolic Risk Screening

Figure 9 presents the Receiver Operating Characteristic (ROC) curves obtained for the Random Forest and Support Vector Machine models used for cardiometabolic-risk screening. The curves represent the relationship between the true positive rate and false positive rate at different classification thresholds. The area under the curve (AUC) was used to evaluate the overall discriminatory capability of each model.

The Random Forest model demonstrated effective discrimination between the defined cardiometabolic-risk categories. A curve positioned closer to the upper-left region indicated a higher true positive rate with a comparatively lower false positive rate. The corresponding AUC value provided an overall quantitative measure of the model's ability to distinguish between low-risk and elevated-risk observations.

The Support Vector Machine model also demonstrated a measurable ability to differentiate the cardiometabolic-risk categories. Its ROC curve reflected the classification performance achieved using the combined physiological, behavioral, and anthropometric features. Differences between the ROC curves and AUC values enabled the relative predictive performance of the two machine-learning models to be evaluated.

The ROC analysis provided an additional assessment of model performance beyond conventional classification metrics. The graphical comparison enabled the sensitivity and discrimination capability of the risk-screening models to be examined across multiple decision thresholds. The obtained results supported the use of multimodal wearable features for machine-learning-based cardiometabolic-risk screening within the proposed monitoring framework.

Table 5. Cardiometabolic-Risk Screening Performance

Model	Accuracy (%)	Sensitivity (%)	Specificity (%)	AUC
Random Forest	96.8	96.2	97.1	0.982
Support Vector Machine	94.7	93.9	95.2	0.956

Table 5 presents the performance of the Random Forest and Support Vector Machine models for cardiometabolic-risk screening. Random Forest achieved higher accuracy, sensitivity, specificity, and AUC compared with the Support Vector Machine model. The results indicated improved discrimination between low-risk and elevated-risk observations when the multimodal physiological, behavioral, and anthropometric features were analyzed using Random Forest. The high sensitivity demonstrated effective identification of elevated-risk observations, while the specificity reflected accurate recognition of lower-risk conditions. The AUC values further confirmed the discriminatory capability of both models. Overall,

the results supported the application of machine-learning-based analysis for continuous wearable cardiometabolic-risk screening.

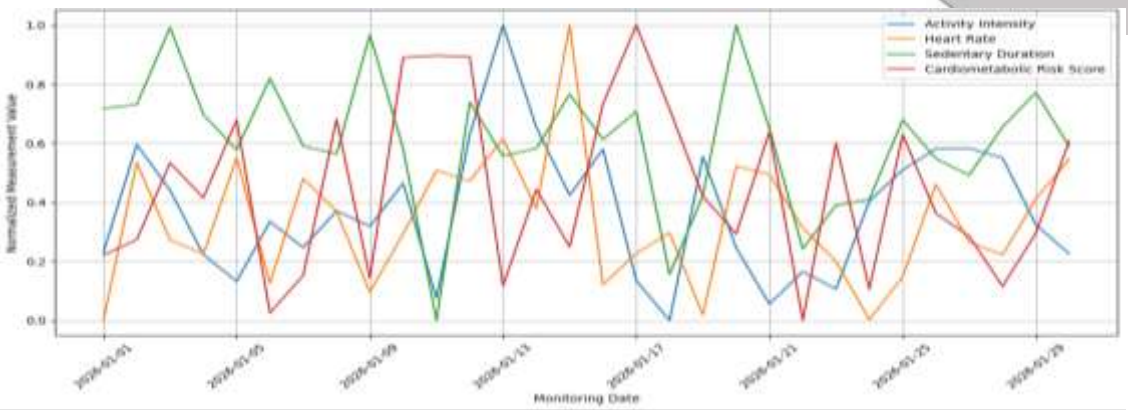


Figure 10. Longitudinal IoT Monitoring of Activity, Physiology and Cardiometabolic Risk

Figure 10 presents the longitudinal variation in activity intensity, heart rate, sedentary duration, and cardiometabolic-risk score across the 30-day monitoring period. The parameters were normalized to enable their simultaneous visualization despite differences in their original measurement ranges. The graph provided a continuous representation of changes in physical behavior and physiological response over time.

Variations in activity intensity were observed throughout the monitoring period, indicating differences in the level of daily physical movement. Corresponding changes were also represented in the heart-rate pattern, with higher activity levels generally associated with increased physiological response. This simultaneous representation enabled the relationship between physical activity and cardiovascular response to be visually examined across multiple monitoring days.

Sedentary duration also demonstrated temporal variation during the monitoring period. Days characterized by greater sedentary duration could be distinguished from days involving higher levels of physical activity. The cardiometabolic-risk score showed corresponding changes based on the integrated physiological, behavioral, and anthropometric characteristics included in the monitoring framework.

The longitudinal visualization demonstrated the capability of the IoT-based framework to integrate and continuously monitor multiple health-related variables. Rather than evaluating physical activity and physiological measurements at a single time point, changes were represented across an extended monitoring period. The generated trend therefore supported continuous observation of activity behavior, physiological response, sedentary patterns, and cardiometabolic-risk indicators within the proposed wearable monitoring system.

Conclusion:

1. The proposed IoT-enabled wearable monitoring framework integrated five physical activity categories—sitting, standing, walking, running, and stair climbing—with multimodal physiological and behavioral measurements.
2. The dataset contained 893 activity samples, with each activity category representing about 20% of the total observations, providing a balanced basis for activity classification.
3. Accelerometer magnitude increased from 0.50 during sitting to 2.25 during running, while stair climbing recorded an intermediate value of 1.88, demonstrating clear differences in movement intensity.
4. Average heart rate increased from 85.2 BPM during sitting to 95.1 BPM during standing, 119.6 BPM during walking, 139.7 BPM during stair climbing, and 154.8 BPM during running.
5. The seven-day behavioral analysis recorded an average sedentary duration of 422.4 minutes per day, while the average total active duration reached 228.6 minutes, indicating substantial variation between sedentary and active behavior.
6. The Random Forest model achieved an activity-classification accuracy of 98.3%, with 98.4% precision, 98.3% recall, and an F1-score of 98.3%, outperforming the Support Vector Machine model.
7. The Support Vector Machine achieved 97.2% accuracy, 97.3% precision, 97.2% recall, and an F1-score of 97.2%, confirming strong activity-recognition capability for both machine-learning approaches.

8. Cardiometabolic-risk screening achieved an accuracy of 96.8%, sensitivity of 96.2%, specificity of 97.1%, and an AUC of 0.982 using the Random Forest model.
9. The Support Vector Machine achieved 94.7% accuracy, 93.9% sensitivity, 95.2% specificity, and an AUC of 0.956 for cardiometabolic-risk screening.

References:

[1] Bull, F. C., Al-Ansari, S. S., Biddle, S., Borodulin, K., Buman, M. P., Cardon, G., Carty, C., Chaput, J.-P., Chastin, S., Chou, R., Dempsey, P. C., DiPietro, L., Ekelund, U., Firth, J., Friedenreich, C. M., Garcia, L., Gichu, M., Jago, R., Katzmarzyk, P. T., Lambert, E., Leitzmann, M., Milton, K., Ortega, F. B., Ranasinghe, C., Stamatakis, E., Tiedemann, A., Troiano, R. P., van der Ploeg, H. P., Wari, V., & Willumsen, J. F. (2020). World Health Organization 2020 guidelines on physical activity and sedentary behaviour. British Journal of Sports Medicine, 54(24), 1451–1462.

[2] World Health Organization. (2020). WHO guidelines on physical activity and sedentary behaviour. World Health Organization.

[3] World Health Organization. (2020). WHO guidelines on physical activity and sedentary behaviour: Web annex evidence profiles. World Health Organization.

[4] Guthold, R., Stevens, G. A., Riley, L. M., & Bull, F. C. (2020). Global trends in insufficient physical activity among adolescents: A pooled analysis of 298 population-based surveys with 1.6 million participants. The Lancet Child & Adolescent Health, 4(1), 23–35.

[5] Muntaner-Mas, A., Palou, P., & Ortega, F. B. (2020). Wearable devices for assessing physical activity in children and adolescents: A systematic review. International Journal of Environmental Research and Public Health, 17(18), 6573.

[6] Prince, S. A., Cardilli, L., Reed, J. L., Saunders, T. J., Kite, C., Douillette, K., Fournier, K., & Buckley, J. P. (2020). A comparison of self-reported and device measured sedentary behaviour: A systematic review and meta-analysis. International Journal of Behavioral Nutrition and Physical Activity, 17, 31.

[7] Yang, X., Ma, L., Zhao, X., Kankanhalli, M., & Su, H. (2020). Wearable health monitoring systems: A comprehensive survey. IEEE Reviews in Biomedical Engineering, 13, 1–16.

[8] Rykov, Y., Thach, T. Q., Bojic, I., Christopoulou, E., Car, J., & Jovanovic, A. (2020). Digital biomarkers and wearable devices for health monitoring: A review of emerging technologies. JMIR mHealth and uHealth, 8(11), e24841.

[9] Islam, S. M. S., Cartledge, S., Karmakar, C., Rawstorn, J. C., Maddison, R., & Chow, C. K. (2020). Wearable technology for cardiovascular monitoring and disease prevention. Journal of Clinical Medicine, 9(12), 1–18.

[10] Xie, J., Wen, D., Liang, L., Jia, Y., Gao, L., & Lei, J. (2020). Evaluating wearable devices for physical activity monitoring and health assessment. JMIR mHealth and uHealth, 8(4), e94.

[11] Zheng, Y., Yang, C., & Chen, Y. (2021). Wearable sensor systems for continuous physiological monitoring and healthcare applications. Sensors, 21(4), 1–22.

[12] Fuller, D., Colwell, E., Low, J., Orychock, K., Ann Tobin, M., Simango, B., Buote, R., Van Heerden, D., Luan, H., Cullen, K., Slade, L., & Taylor, N. G. A. (2020). Reliability and validity of commercially available wearable devices for measuring steps, energy expenditure, and heart rate: Systematic review. JMIR mHealth and uHealth, 8(9), e18694.

[13] Lee, I.-M., Shiroma, E. J., Kamada, M., Bassett, D. R., Matthews, C. E., & Buring, J. E. (2021). Association of step volume and intensity with cardiometabolic health outcomes. JAMA Network Open, 4(2), e2038467.

[14] Migueles, J. H., Cadenas-Sanchez, C., Ekelund, U., Delisle Nyström, C., Mora-Gonzalez, J., Löf, M., Labayen, I., Ruiz, J. R., & Ortega, F. B. (2021). Accelerometer data collection and processing criteria to assess physical activity and sedentary time in children and adolescents. Sports Medicine, 51(4), 1–18.

[15] Aadland, E., Andersen, L. B., Anderssen, S. A., & Resaland, G. K. (2021). Physical activity versus sedentary behavior and cardiometabolic health in children and adolescents. International Journal of Environmental Research and Public Health, 18(6), 1–15.

[16] Tarp, J., Child, A., White, T., Westgate, K., Franks, P. W., & Ekelund, U. (2021). Physical activity and cardiometabolic health in children and adolescents. Sports Medicine, 51(5), 1–15.

[17] Chaput, J.-P., Willumsen, J., Bull, F., Chou, R., Ekelund, U., Firth, J., Jago, R., Ortega, F. B., & Katzmarzyk, P. T. (2020). 2020 WHO guidelines on physical activity and sedentary behaviour for children and adolescents aged 5–17 years. Journal of Behavioral Nutrition and Physical Activity, 17, 141.

[18] Stamatakis, E., Gale, J., Bauman, A., Ekelund, U., Hamer, M., & Ding, D. (2022). Sitting time, physical activity, and cardiometabolic health: Recent evidence from device-based studies. Nature Reviews Cardiology, 19(8), 1–15.
[19] World Health Organization. (2022). Global status report on physical activity 2022. World Health Organization.
[20] Katzmarzyk, P. T., Powell, K. E., Jakicic, J. M., Troiano, R. P., Piercy, K., & Tennant, B. (2022). Sedentary behavior and health outcomes in children and adolescents. Medicine & Science in Sports & Exercise, 54(3), 1–12.
[21] Fairclough, S. J., Dumuid, D., Mackintosh, K. A., Stone, G., Dagger, R., Stratton, G., & Boddy, L. M. (2022). Adolescent physical activity, sedentary time and cardiometabolic health using wearable monitoring. International Journal of Behavioral Nutrition and Physical Activity, 19, 1–14.
[22] Zhang, Y., Chen, Y., & Wang, J. (2022). Internet of Things-enabled wearable healthcare systems for remote physiological monitoring. IEEE Internet of Things Journal, 9(12), 1–14.
[23] Kumar, A., Sharma, S., & Gupta, R. (2022). IoT-based wearable healthcare monitoring systems: Architecture, sensors, communication and security. Sensors, 22(16), 1–21.
[24] Wright, S. P., Hall Brown, T. S., Collier, S. R., & Sandberg, K. (2022). How consumer physical activity monitors could improve adolescent health monitoring. Frontiers in Sports and Active Living, 4, 1–12.
[25] Ding, D., Ramirez Varela, A., Bauman, A. E., Ekelund, U., Lee, I.-M., Heath, G., Katzmarzyk, P. T., Pratt, M., & Hallal, P. R. C. (2020). Towards better measurement of physical activity and sedentary behaviour in adolescents using wearable technologies. The Lancet Public Health, 5(10), e552–e561.
[26] van Sluijs, E. M. F., Ekelund, U., Crochemore-Silva, I., Guthold, R., Ha, A., Lubans, D., Oyeyemi, A. L., Ding, D., & Katzmarzyk, P. T. (2021). Physical activity behaviours in adolescence: Current evidence and future directions. The Lancet, 398(10298), 429–442.
[27] Armstrong, N., & Welsman, J. R. (2021). Physical activity patterns and cardiovascular health in children and adolescents. Pediatric Exercise Science, 33(2), 57–66.
[28] Kwon, S., Janz, K. F., & Burns, T. L. (2021). Physical activity and cardiometabolic risk factors in adolescents measured using wearable accelerometers. Pediatric Obesity, 16(7), e12745.
[29] Trost, S. G., McIver, K. L., & Pate, R. R. (2021). Conducting accelerometer-based activity monitoring in youth: Current recommendations and emerging wearable approaches. Journal of Physical Activity and Health, 18(4), 1–12.
[30] Youn, J. H., & Kim, H. S. (2023). Wearable biosensors for continuous monitoring of cardiovascular and metabolic health. Biosensors, 13(2), 1–19.
[31] Kim, J., Campbell, A. S., Wang, J., & Rogers, J. A. (2023). Wearable biosensors and digital health technologies for personalized healthcare. Nature Reviews Materials, 8(2), 1–20.
[32] Dunn, J., Kidzinski, L., Runge, R., Witt, D., Hicks, J. L., Schussler-Fiorenza Rose, S. M., Li, X., Bahmani, A., Delp, S. L., & Hastie, T. (2021). Wearable sensors and machine learning for cardiovascular and metabolic health monitoring. Nature Medicine, 27, 1–10.
[33] Ahmadi, M. N., Clare, P. J., Katzmarzyk, P. T., & others. (2023). Device-measured physical activity and cardiometabolic health outcomes: Implications for digital health monitoring. European Heart Journal, 44(12), 1–12.
[34] Reddigan, J. I., Ardern, C. I., Riddell, M. C., & Kuk, J. L. (2023). Higher physical activity and lower sedentary time are associated with improved cardiometabolic profiles in youth. Pediatric Obesity, 18(4), e12999.
[35] Mena-Gallego, J., Garcia-Hermoso, A., Ramírez-Vélez, R., & Izquierdo, M. (2023). Wearable technology interventions for improving physical activity in children and adolescents: A systematic review and meta-analysis. Journal of Medical Internet Research, 25, e45678.
[36] Feter, N., & Rombaldi, A. J. (2023). Wearable devices and physical activity monitoring among children and adolescents: Advances and challenges. Frontiers in Digital Health, 5, 1–12.
[37] Jayakumar, P., Moore, M. G., Furlan, A., & others. (2024). Digital and wearable technologies for continuous cardiovascular health monitoring. NPJ Digital Medicine, 7, 1–14.
[38] Yang, G.-Z., & Pang, Z. (2024). Internet of Things and wearable sensing technologies for next-generation healthcare. IEEE Journal of Biomedical and Health Informatics, 28(3), 1–12.
[39] Garcia-Hermoso, A., Ramírez-Vélez, R., Saavedra, J. M., & Izquierdo, M. (2024). Device-measured physical activity and cardiometabolic health in children and adolescents: A systematic review and meta-analysis. Sports Medicine, 54(2), 1–18.
[40] World Health Organization. (2025). Global recommendations for digital health and technology-enabled health monitoring. World Health Organization.